GEOLOGIC/GEOMORPHOLOGIC MAPPING OF A COMPLEX IMPACT CRATER IN THE NORTHERN PLAINS OF MARS. P. Jodłowski, C. Gross, L. Wendt, P. Halbach, G. Neukum, Freie Universität Berlin, Institute of Geological Sciences, Planetary Sciences and Remote Sensing; Malteserstr. 74–100, D–12249 Berlin, Germany; piotr.jodlowski@fu–berlin.de

Introduction: Detailed maps are needed to correlate hyperspectral data obtained by the Compact Reconnaissance Imaging Spectrometer for Mars (CRISM) and processed with methods described in [1] with geomorphologic units within selected craters. Phyllosilicates are of particular interest, because they require long–lasting liquid water abundance in order to precipitate [2]. Such conditions were met in the early history of Mars, in the Noachian period. As most of the phyllosilicate outcrops are found in depressions, valleys or impact craters, predominantly in Noachian strata, it leads to conclusion that they must be excavation products of preexisting buried deposits, exposed by impacting, faulting or erosion [3, 4]. However, combined spectral and geomorphologic data [2] and [5] have shown that the Hesperian–aged Toro crater (17.0° N, 71.8° E) bears evidence for impact–induced hydrothermal mineralizations, extending phyllosilicate synthesis to post–Noachian times. This work will give insight into the geomorphology of a phyllosilicate–bearing, unnamed crater, located in the northern lowlands of Mars.

Geologic Setting and Study Area: The crater is located in the northern hemisphere, roughly 400–500 km north of the dichotomy boundary, in the Vastitas Borealis Formation (Northern Plains) at 50°33’5,08”N 16°20’20,37”E, east of Acidalia Planitia and ca. 500 km to the west of the double–ringed Lyot crater. It is overlying the Early Amazonian Vastitas Borealis interior unit [6]. The crater has a diameter of ~50 km and a maximal depth of ~4.3 km below the reference. The base of the crater is located at ~3 km below the topographic datum. The major axis of the asymmetrical central uplift complex is ~20 km long and the minor axis ~18 km.

Data Sets and Methods: The intention was to provide a geomorphologic map in reasonably highest detail, which requires data with the highest coverage–to–ground resolution ratio. Therefore, HRSC data from orbit 3304 with 12.5 m/px and CTX image B01_009997_2308_XN_50N343W with 6.1 m/px were used as the mapping basis. In addition HiRISE image ESP_016577_2310 was used for the identification of particular textural properties of the surface units, but was not used for the mapping itself.

Image processing was conducted in ISIS3 environment and the mapping in ESRI’s ArcGIS 9.3 with additional usage of File Geodatabase.

The main decisive factor in the process of unit identification, distinction and mapping was the morphology, understood as the product of surface’s roughness, albedo, form and optional special features contributing to the general appearance. Mineralogical composition did not play any role in either identification or mapping processes.

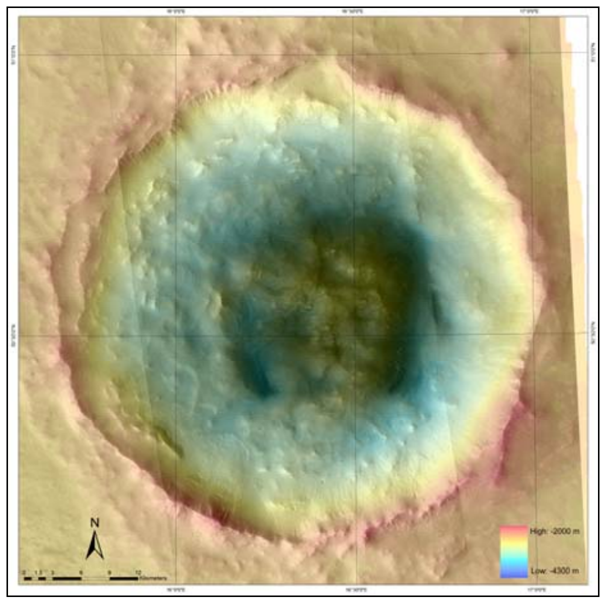

Figure 1: HRSC orbit 3304 with 12.5 m/px and CTX image B01_009997_2308_XN_50N343W with 6.1 m/px overlaid by color-coded elevation data derived from HRSC’s stereo channels.

Observations: The studied crater was roughly divided into three main mapping–sections, each characterized by the occurrence of particular units.

Peak ring area. Most of the inner part of the crater is characterized by significantly lower albedo, well developed peak ring structure [7] with varied, but mostly rough, surfaces and two large dark–colored dune fields in the SW and E, at the transitional boundary to the second section. Fan deposits, light–toned fine material and light–toned linear dunes were also identified. Several linear features were mapped, including gullies and ridges.

Outer ring area. This section is placed between the peak ring area and the crater rim. It shows a higher albedo and more smoothed appearance than the peak ring area. Its most prominent feature is the predominant occurrence of various types of dissected mantle terrains [8]. Terrains adjacent to the peak ring area were classified as pitted and patterned surfaces. The degree of erosion increases towards the crater rim, resulting in knobby and wavy surfaces, with occasional scallops. Other features are very smooth surfaced depression fillings and terraces [7].

Crater rim area. This section covers the surfaces adjacent or closely associated with the rim: the crater rim surface unit itself and landslides. The first describes the slope of the rim, which was not modified in any way. Its outer boundary reaches the base surface of the studied crater. Landslides occur mainly in the eastern part of the area. The most prominent is ~6 km long.

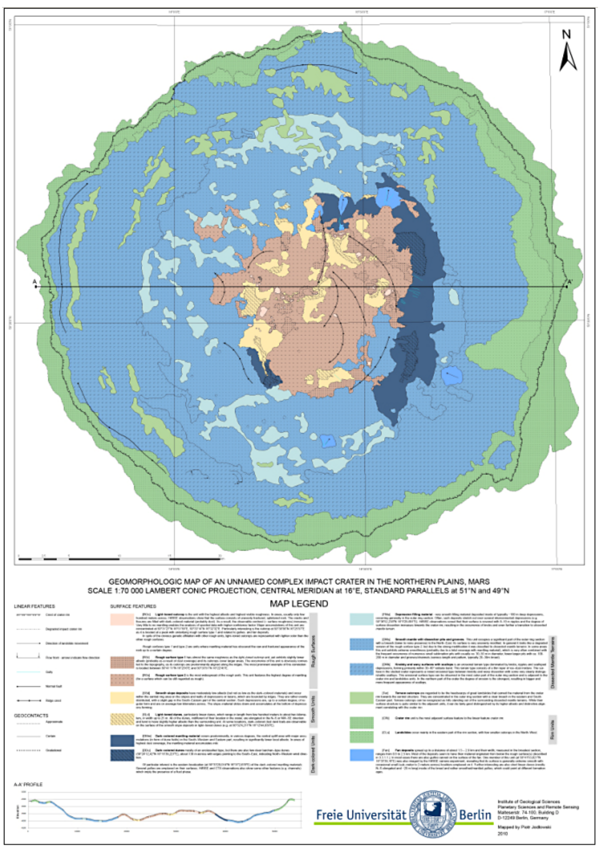

Conclusions and Discussion: In total, 14 surface units and 7 linear units were mapped. In this study, the occurrence of gullies and fan deposits is of crucial importance, as they are evidence for liquid water [9], which is an essential requirement for the phyllosilicate precipitation [2, 3]. The correlation of mapped units with spectral data obtained by CRISM and OMEGA will allow the validation of existing theories on hydrothermal processes and mineral precipitation in impact craters [2, 5]. In this process, the presence of distinctive surface mantling, in various erosional degrees, must be taken into account as a factor obscuring the original material or even interacting with it.

Figure 2: Geologic/geomorphologic map of the investigated crater. The mapping was carried out at a scale of 1:30.000.

Outlook: As a next step, other phyllosilicate–bearing impact craters in the Martian Northern Plains will be mapped. Further, craters in mid and southern latitudes are envisaged for mapping, in order to compare their results with those from the northern latitudes. Studying the differences and similarities of such craters will provide additional information on the presence or absence of water in different stratigraphic units of Mars and the influence of mantling material on the identification of hydrous minerals.

Acknowledgements: This work has been supported by the DFG Grant NE 212/11–1, by the Helmholtz Association through the research alliance "Planetary Evolution and Life" and by the German Space Agency (DLR Bonn) grant 50QM1001 (HRSC on Mars Express), on behalf of the German Federal Ministry of Economics and Technology. Additionally we would like to thank A. Dumke for the HRSC–DTM processing.

References: [1] Gross C. (2011) *42nd LPSC, The Woodlands, Texas.* [2] Fairén A. G. et al. (2010) *Proc. Natl. Acad. Sci. 107 (27),* 12095–12100. [3] Bibring J.–P. et al. (2006) *Science, 312*, 400. [4] Murchie S. L. et al. (2006) *J. Geophys. Res., 114,* E00D07. [5] Marzo G. A. et al. (2010) *Icarus, 208,* 667–683. [6] Tanaka et al. (2005) SIM 2888, USGS. [7] Melosh H. J. (1989) *Oxford Monogr. on Geol. And Geoph. No.11.* [8] Milliken R. E. et al. (2003) *6th Int. Conf. on Mars*, Abstract #3240. [9] Malin et al. (2000) *Science, 288*, 2330–2335.